Water Air Soil Pollut (2025) 236:574
https://doi.org/10.1007/s11270-025-08223-4

Chitosan-Derived Porous Carbon for Efficient Adsorptive Removal of Amoxicillin and Doxycycline Antibiotics from Aqueous Systems

Feride N. Türk · Hasan Arslanoğlu

Received: 31 March 2025 / Accepted: 29 May 2025 / Published online: 10 June 2025

Abstract Traditional antibiotic removal techniques—such as coagulation, membrane filtration, ozonation, and biodegradation—are often inadequate for large-scale applications due to limiting factors including high operational costs, complex system design, and the formation of toxic by-products. In addition, the low selectivity levels of these techniques and the need for additional post-treatment make it difficult to achieve effective and sustainable water treatment goals. The phosphoric acid-activated chitosan-derived carbon adsorbent proposed in this study demonstrated superior adsorption capacities for both amoxicillin and doxycycline, owing to its high surface area and abundant functional groups, aligning with sustainability principles. Thus, it stands out as an economical and environmentally friendly alternative that directly solves the shortcomings of previous methods. High-performance activated carbon was synthesized via phosphoric acid activation of chitosan for the removal of amoxicillin (AMX) and doxycycline (DOC) antibiotics from aqueous solutions. The adsorption efficiency was systematically evaluated in batch experiments at temperatures ranging from 30 to 50 °C, initial antibiotic concentrations of 50–400 mg/L, and pH levels spanning from 3 to 13. The phosphoric acid activation process significantly influenced the physicochemical properties of the resultant activated carbon, enhancing its structural and textural characteristics. The activated carbon exhibited a substantial surface area of 998.02 m^2/g, a pore volume of 0.485 cm^3/g, and an average pore diameter of 2.55 nm, structure favorable for adsorption. Furthermore, kinetic analysis revealed that the adsorption process followed the pseudo-first-order model, indicating that physisorption was the dominant mechanism. Equilibrium data were best described by the Langmuir isotherm model, highlighting monolayer adsorption on a homogeneous surface. The maximum adsorption capacities for AMX and DOC were determined to be 227.18 mg/g and 299.07 mg/g, respectively, at 50 °C, demonstrating the high affinity of the adsorbent for these pharmaceutical contaminants. These findings indicate that chitosan-derived activated carbon is a cost-effective, sustainable material with strong potential for removing antibiotic contaminants from wastewater.

Keywords Activated carbon · Activation · Adsorption · Antibiotics · Chitosan

F. N. Türk
Central Research Laboratory Application and Research Center, Çankırı Karatekin University, Çankırı 18100, Turkey
e-mail: ferideturk23@gmail.com

H. Arslanoğlu (✉)
Department of Chemical Engineering, Çanakkale Onsekiz Mart University, Engineering Faculty, 17020 Çanakkale, Turkey
e-mail: hasan.arslanoglu@comu.edu.tr

1 Introduction

The contamination of water bodies with pharmaceuticals, particularly antibiotics, has become a growing environmental concern due to their extensive global usage in medical and veterinary applications (Baccar et al., 2012). Antibiotics such as amoxicillin (AMX) and doxycycline (DOC) are commonly used to treat bacterial infections, however, their continuous release, hospitals, and households results in their accumulation in aquatic ecosystems, posing risks such as bacterial resistance, toxicity, and ecological imbalance (Bagheri et al., 2016; Kimura et al., 2005). AMX, a β-lactam antibiotic, has been associated with the emergence of resistant bacterial strains and adverse effects such as skin diseases and environmental odor issues (Tiwari et al., 2017). Similarly, making its removal from water sources even more essential from water sources (Rocha et al., 2020).

In this study, amoxicillin (AMX) and doxycycline (DOC), which were selected as model pollutants, were preferred not only because of their widespread use but also because of the significant differences they exhibit in terms of their chemical structures, polarities and environmental persistence profiles. AMX is a semi-synthetic penicillin derivative containing a β-lactam ring and is known for its high solubility in water and moderate polarity. In contrast, DOC is a broad-spectrum antibiotic belonging to the tetracycline group and is more resistant to environmental conditions with its polyphenolic structure, high degree of conjugation and amphoteric character. These two molecules show different properties in terms of hydrogen bonds, electrostatic interactions and π-π interactions that affect the adsorption mechanisms. Therefore, considering both antibiotics together in this study is important in terms of evaluating the selectivity and efficiency of the developed adsorbent against multiple structural pollutants. In addition, comparing the removal behaviors of antibiotics with different molecular properties provides a more holistic perspective in terms of mechanistic modeling and adsorption efficiency (Kümmerer, 2009; Martínez-Carballo et al., 2007; Watkinson et al., 2007).

Several techniques, including coagulation, membrane filtration, ozonation, and biodegradation, have been explored for antibiotic removal; however, their high operational costs, technical complexity, and formation of hazardous byproducts limit their large-scale application (Sánchez-Polo et al., 2008; Zhang et al., 2011). Adsorption, particularly using activated carbon (AC), has emerged as an efficient and cost-effective alternative due to its high surface area, well-developed porosity, and ability to remove trace contaminants without generating secondary pollutants (Martins et al., 2017; Tambosi et al., 2010). ACs derived from natural, agricultural, and industrial waste materials provide a sustainable solution by transforming waste into valuable adsorbents while mitigating environmental disposal issues (Naghdi et al., 2018).

Chitosan (CS), a biopolymer obtained through the deacetylation of chitin, is an excellent precursor for AC synthesis due to its high carbon content, cationic nature, and abundance in marine waste streams (Silva Alves et al., 2021; Wróbel-Iwaniec et al., 2015). The global annual production of chitin exceeds 1,300 million tons, and its conversion into CS-based adsorbents offers an eco-friendly and economically viable strategy for water treatment (Liu et al., 2018). The presence of amino and hydroxyl functional groups in CS enhances adsorption efficiency by providing active binding sites for pollutants (Kumar et al., 2022).

In previous studies, most of the biomass sources used in activated carbon production have significant limitations in terms of process efficiency, surface area development and cost-effectiveness, although they exhibit good adsorption properties due to their lignocellulosic content. For example, although agricultural residues (such as rice husk, hazelnut shell, corn cob) are widely used, the surface areas of activated carbons obtained from these raw materials are generally limited and strong chemical activators (e.g. KOH, $ZnCl_2$) are needed to reach higher surface areas. This situation creates both negative environmental effects and increases production costs (Bhatnagar & Sillanpää, 2010; Ioannidou & Zabaniotou, 2007). However, although high surface area (> 1000 m^2/g) is obtained in some methods, the adsorption efficiency remains low for the targeted pollutants or selective adsorption cannot be achieved due to insufficient surface functional groups. In addition, optimizations in parameters such as pyrolysis temperature and activation time are generally energy intensive and create difficulties in terms of portability to industrial scale (Foo & Hameed, 2012).

Various activation methods have been employed to enhance the porosity and adsorption properties of CS-based ACs. Alkaline activation with NaOH facilitates mesoporous carbon formation, effectively removing large synthetic dyes (Sun, et al., 2016). Zinc chloride ($ZnCl_2$) activation has also been used, but its high corrosiveness and environmental risks limit its application (Fan et al., 2020). In contrast, phosphoric acid (H_3PO_4) activation is considered a more sustainable and cost-effective approach, as it operates at lower temperatures, exhibits minimal corrosive effects, and does not introduce residual metal contaminants into the final product (Antonelli et al., 2020).

Conventional removal techniques, including coagulation, membrane filtration, and biodegradation, face challenges such as high costs, technical complexity, and toxic byproduct formation. Adsorption, particularly using activated carbon (AC), is a highly effective alternative due to its high surface area, functionalized adsorption sites, and cost-effectiveness.

Chitosan (CS), a biodegradable and abundant biopolymer derived from chitin, is a promising precursor for AC production. Its amino and hydroxyl functional groups enhance adsorption performance, making it an environmentally safe sorbent. Various activation methods have been used to improve CS-based ACs, including NaOH and $ZnCl_2$ treatments, though these may pose economic and environmental concerns. Phosphoric acid (H_3PO_4) activation presents a more sustainable and cost-effective approach, offering lower processing temperatures, reduced equipment corrosion, and minimal residue formation. This study focuses on synthesizing chitosan-derived activated carbon (CS-AC) via single-step H_3PO_4 activation and evaluating its adsorption efficiency for AMX and DOC removal.The findings will contribute to the development of environmentally friendly and highly efficient adsorbents for pharmaceutical wastewater treatment, addressing both pollution control and waste valorization challenges.

2 Experimental

2.1 Materials

Chitosan flakes were acquired from Agada Chemical, Türkiye. Amoxicillin (AMX, $C_{16}H_{19}N_3O_5S$, 365.4 g/mol) and doxycycline (DOC, $C_{22}H_{24}N_2O_8$, 444.43 g/mol) were sourced from a pharmaceutical distributor in Türkiye. Phosphoric acid (H_3PO_4) with approximately 99% purity, along with other analytical-grade reagents, was obtained from Sigma-Aldrich.

2.2 Structural Analysis of CS–AC

Activated carbon (AC) was synthesized from chitosan (CS) through a single-step phosphoric acid activation process in a batch setup. Specifically, 40 g of CS flakes were impregnated with a designated volume of 25 wt% concentrated H_3PO_4 under intermittent stirring. The resulting slurry was subjected to drying at 100 °C for 12 h. The dried material was then pyrolyzed in a cylindrical reactor under a nitrogen flow of 100 cm^3/min at 600 °C, with a heating rate of 10 °C/min, for a duration of 90 min. After activation, the obtained samples were cooled to ambient temperature, thoroughly rinsed with hot distilled water (65 °C) until the pH stabilized between 6 and 7, and subsequently oven-dried at 100 °C for 48 h before being stored in airtight plastic containers.

The structural and textural characteristics of the synthesized CS-derived activated carbon (CS–AC) were analyzed using various techniques. Surface morphology was examined via scanning electron microscopy (SEM) using a Zeiss Supra. The specific surface area and pore properties were determined using the Brunauer–Emmett–Teller (BET) theory and the Barrett–Joyner–Halenda (BJH) method, utilizing a Micromeritics ASAP 2020 analyzer. Functional groups present on CS–AC, both before and after interaction with antibiotics, were identified through Fourier transform infrared (FTIR) spectroscopy.

2.3 Adsorption Efficiency of CS–AC

The adsorption efficiency of CS–AC for the removal of AMX (Amoxicillin) and DOC (Doxycycline) was assessed by considering the influence of several factors such as initial antibiotic concentrations, contact times, and solution pH levels. To determine this efficiency, the following experimental procedure was followed:

Initial Antibiotic Concentrations and Contact Time: 200 mL of AMX or DOC solutions with varying initial concentrations ranging from 50 mg/L to 400 mg/L were placed in a 250 mL conical flask equipped with a stopper. To this flask, 0.2 g of

CS–AC was added, and the mixture was agitated at 140 rpm in a water shaker maintained at a constant temperature of 30 °C. The system was kept under different contact times to analyze the impact of the initial concentration and contact time on the adsorption efficiency. Effect of pH: For studying the effect of pH, 100 mL of AMX or DOC solution, with an initial concentration of 100 mg/L, was placed in a conical flask (250 mL). To this solution, 0.10 g of CS–AC was added, and the flask was agitated at different pH levels, ranging from 3 to 13. The system was incubated for 30 h at 30 °C to observe how different pH levels influenced the adsorption efficiency. Isotherm Study: To study the adsorption isotherm, the system was allowed to reach equilibrium at various temperatures ranging from 30 °C to 50 °C. The adsorption data obtained at different temperatures were used to determine the equilibrium adsorption capacity and to model the adsorption isotherm. Kinetic Study: During the kinetic study, the concentration of AMX or DOC was measured at different time intervals (from 0 to 30 h) until equilibrium was reached. The adsorption capacity, qt (mg/g), of CS–AC at time t was calculated using the following equation:

$$q_t = \frac{(C_0 - C_t) \times V}{W} \quad (1)$$

where: C_0 is the initial concentration of the antibiotic (mg/L), C_t is the concentration of the antibiotic at time t (mg/L), V is the volume of the antibiotic solution (L), W is the mass of CS–AC (g). Quantitative Determination:The residual concentration of AMX or DOC was determined by measuring the absorbance using a UV-1200/Visible spectrophotometer at specific wavelengths of 272 nm for AMX and 345 nm for DOC. This procedure allowed for the analysis of how varying initial concentrations, pH conditions, and contact times, as well as the temperature variations, impacted the adsorption efficiency of CS–AC for AMX and DOC.

3 Results and Discussion

3.1 Analysis of CS–AC Structure

The porous nature of the synthesized CS–AC was characterized using nitrogen adsorption isotherms (Fig. 1a), which correspond to a type I isotherm pattern based on IUPAC classification. Type I isotherms are indicative of microporous materials, and the absence of a hysteresis loop suggests minimal mesoporosity (Avcı et al., 2020). As depicted in Fig. 1b, the produced activated carbon exhibits a well-defined pore diameter profile, with dominant pores measuring 2.55 nm in size. The high porosity of the carbonaceous adsorbent enhances the adsorption of organic compounds due to the pore-filling effect, while its microporous structure with a narrow pore size distribution facilitates the uptake of small- to medium-sized drug molecules (Boudrahem et al., 2017).

The specific surface area and pore properties of the synthesized CS–AC were measured as 998.02 m^2/g, 0.485 cm^3/g, and 2.55 nm, respectively. The use of H_3PO_4 as an activating agent significantly enhances the pore structure compared to NaOH-activated CS, which has been previously reported to exhibit a surface area of 358.90 m^2/g and a pore volume of 0.275 cm^3/g (Sun, et al., 2016). The superior porosity of CS–AC can be attributed to the micropore-generating ability of phosphoric acid, which promotes the formation of a high-density microporous network.

The SEM images of CS–AC at different magnifications are displayed in Fig. 2, revealing a heterogeneous, irregular, and highly porous structure with numerous cavities. These cavities facilitate the diffusion of pollutants to the adsorption sites, enhancing the material's adsorption capacity. The formation of the highly porous network is attributed to the internal etching effect of H_3PO_4 as an activating agent (Kong et al., 2017). Quantitative SEM Description:To enhance clarity, we have included quantitative estimates in our SEM image interpretation. Specifically, we added:

> "The observed pore structures in the SEM images ranged approximately from 50 nm to 200 nm in diameter, suggesting a predominance of mesopores with partially collapsed microchannels."

Figure 3 illustrates the active functional groups present on the CS–AC surface before and after antibiotic adsorption. The broad band at 3428.6 cm^{-1} corresponds to -OH groups, which originate from carboxylic acids, alcohols, and phenols (Lu et al., 2018). A weak absorption band at 2305.7 cm^{-1} is associated with C≡N groups of nitriles. The moderate

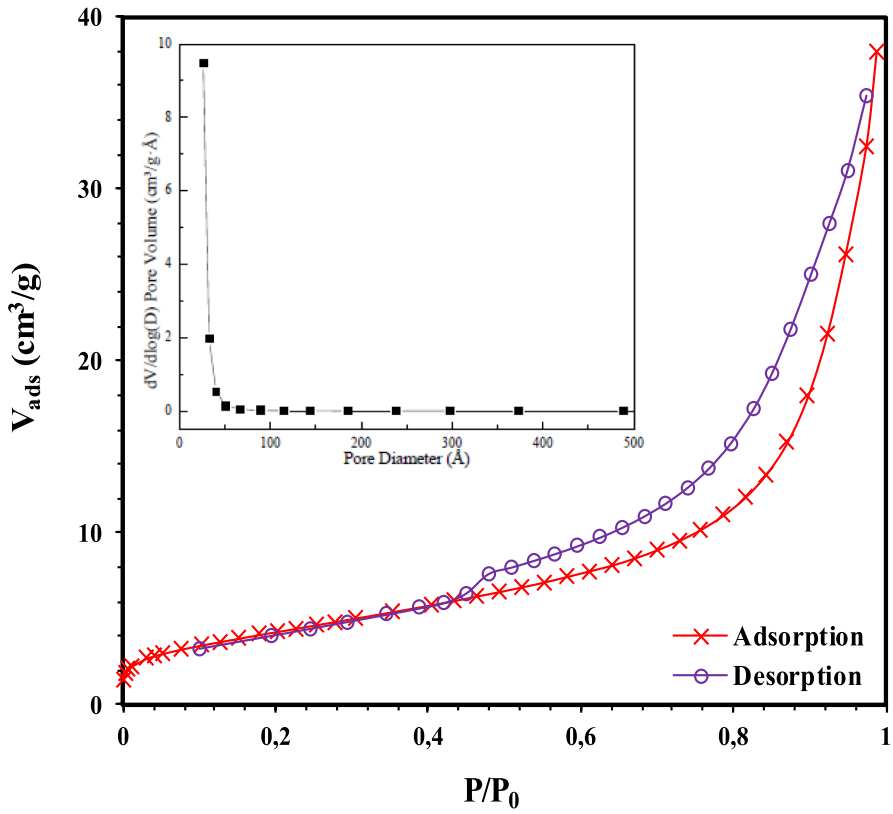

Fig. 1 Nitrogen adsorption–desorption isotherm of CS–AC

peak at 1654.2 cm^{-1} is assigned to N–H stretching, characteristic of primary amines derived from amino groups within the CS structure (Sun, et al., 2016). Additionally, the peak at 1382.1 cm^{-1} corresponds to –CN groups, while the successive bands at 1152.5 cm^{-1} and 1086.9 cm^{-1} indicate the presence of –CN and C–O functional groups (Fan et al., 2013; Zhang et al., 2016a). Overall, the dominance of –CN, O–H, and N–H groups on the CS–AC surface significantly enhances its adsorption potential. Following antibiotic interaction, notable shifts, intensity variations, and disappearances of some peaks are observed (Fig. 3). Specifically, the characteristic bands at 2305.7, 1152.5, and 1086.9 cm^{-1} vanish, while the intensity of the –CN or C–O groups is altered. Additionally, the O–H and N–H bands, initially at 3428.6 cm^{-1} and 1654.2 cm^{-1}, shift to 3450.1 cm^{-1} and 1673.4 cm^{-1}, respectively. These spectral modifications confirm the crucial role of these functional groups in the adsorption process of AMX and DOC onto the CS–AC surface (Liu et al., 2022). FTIR Band Shifts and Molecular Interactions: The FTIR analysis section has been expanded to clarify that the shifts in –OH and –NH stretching vibrations may be attributed to hydrogen bonding and electrostatic interactions between functional groups on the adsorbent surface and the antibiotic molecules (AMX and DOC). These explanations are supported by recent literature.

Zeta potential (ζ-potential) measurements are very important in understanding the charge change of the adsorbent surface depending on pH. The pHpzc (zero point of charge) value obtained in this study was determined as 5.9. It is accepted that the adsorbent surface is positively charged at pH conditions below this value and negatively charged at pHs above it. This directly affects the selectivity of the adsorbent against ionic contaminants. For example, antibiotics such as AMX (amoxicillin) and DOC (doxycycline) can exist in different ionic forms depending on the pH of the solution. While AMX is mostly neutral or slightly anionic in the pH range of 5–7, DOC can exhibit ionic imbalances in a wider pH range. The adsorbent surface, which becomes negatively charged above the pHpzc value, is more prone to electrostatic interactions with positive AMX and DOC species. However, beyond ionic interactions, the actual

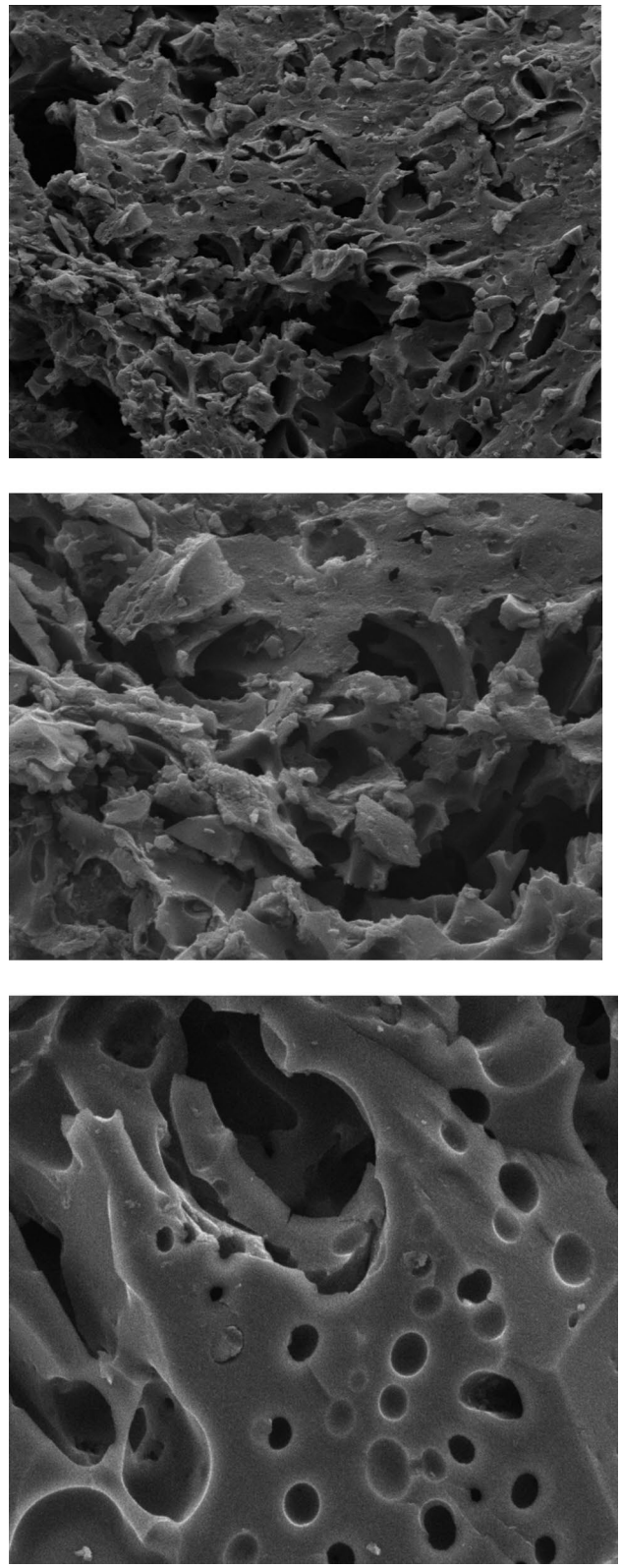

Fig. 2 SEM images of CS–AC at various magnifications

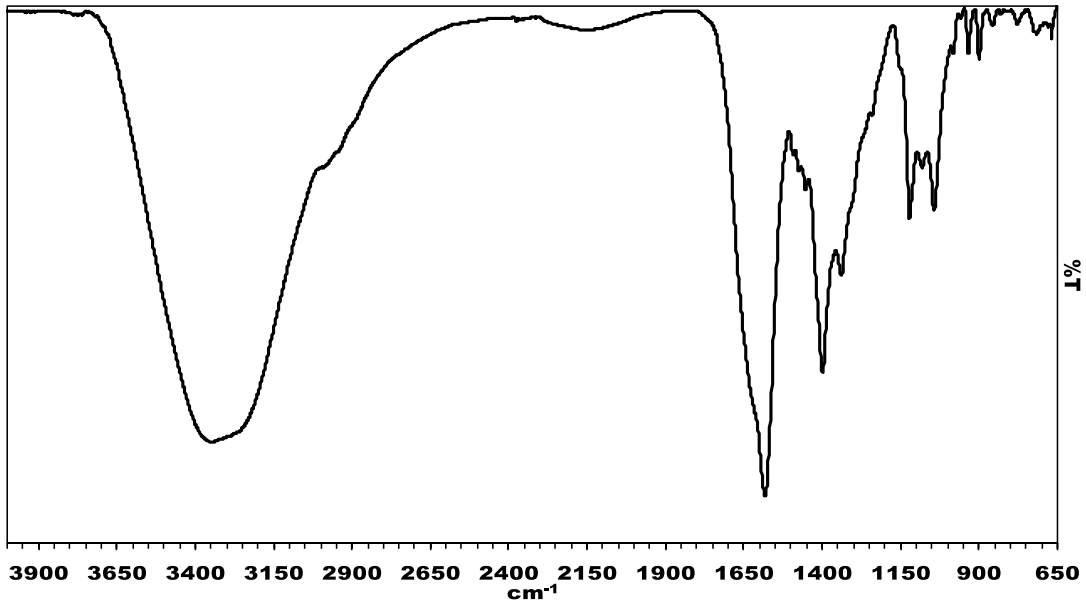

Fig. 3 FTIR spectra of CS–AC before adsorption

efficiency of adsorption is also related to chemical bonds established with surface functional groups and weak physical interactions. The findings obtained from FTIR analyses provide important clues about the adsorption mechanism. The shifts in the characteristic FTIR bands of functional groups such as –OH, $–NH_2$ and –COOH after AMX and DOC adsorption and the disappearance or weakening of some bands indicate that these groups act as active adsorption centers. It is understood that weak interactions, especially hydrogen bonds (e.g. –OH…O = C), π–π interactions (electron cloud overlap between aromatic rings) and van der Waals forces, are effective in binding molecules to the surface. For example, it has been stated in many studies that π–π stacking and hydrogen bonds are effective together in the adsorption of β-lactam antibiotics with similar structures to activated carbon surfaces (Zhang et al., 2020; Yang et al., 2019). In addition, multi-ring systems such as DOC are more prone to π–π interactions with aromatic carbon materials (Zhao et al., 2022). After adsorption, the bands that broaden and shift, especially in the range of 3400–3200 cm^{-1} in FTIR, confirm that –OH and –NH groups participate in hydrogen bonds. Similarly, the changes in the bands belonging to aromatic C = C vibrations in the range of 1600–1500 cm^{-1} are shown as evidence of π–π interactions. As a result, when the zeta potential value and FTIR analyses are evaluated together, it is clearly revealed that physical–chemical interactions such as hydrogen bonds, π–π interactions and dispersion forces via functional groups on the adsorbent surface are effective in the removal of antibiotics as much as electrostatic attraction. This multimodal interaction mechanism supports that the adsorbent is a high-performance and versatile pollutant removal material (Yang et al., 2019; Zhang et al., 2020; Zhao et al., 2022).

3.2 Effect of İnitial pH

The relationship between the adsorption efficiency of CS–AC and the initial pH (3–13) of AMX and DOC solutions, with an inlet concentration of 100 mg/L, is illustrated in Fig. 4. The uptake of AMX increases from 52 to 59 mg/g as the pH rises from 3 to 7 but then declines to 48 mg/g at pH 13. AMX exists in cationic form at pH < 3.5, remains neutral between pH 3.5–7.5, and transitions to an anionic form at pH > 7.5 (Putra et al., 2009). Consequently, the enhanced adsorption observed in the pH range of 3–7 cannot be solely attributed to electrostatic interactions, indicating that hydrogen bonding likely plays a key role in the adsorption mechanism (Tseng, 2006). The reduction in adsorption capacity at pH levels above 7 can

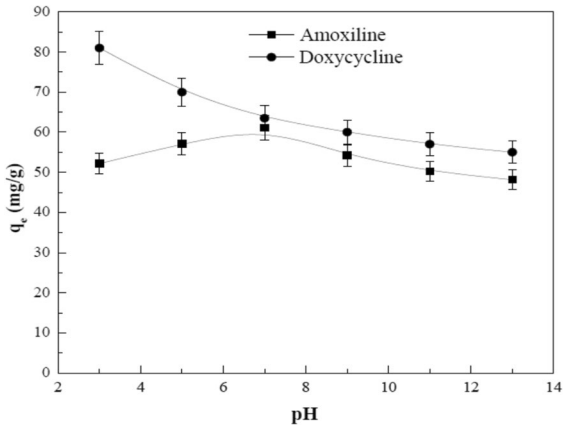

Fig. 4 Effect of solution pH on the uptake of AMX and DOC by CS–AC (dosage: 1 g/L, initial antibiotic concentration: 100 mg/L, agitation speed: 300 rpm, temperature: 30 °C)

be ascribed to repulsive interactions between the negatively charged CS–AC surface and AMX anions (Mangla et al., 2022). For DOC, adsorption capacity declines as pH increases. At pH 3, the uptake is highest (82 mg/g) and decreases to 55 mg/g at pH 11. DOC is cationic at pH < 3.5, neutral in the range of pH 3.5–7.7, and anionic at pH > 7.7 (Chao et al., 2014). The elevated adsorption of DOC under acidic conditions (pH = 3) can be attributed to Van der Waals forces or dipole–dipole interactions between cationic DOC species and the positively charged CS–AC surface. Between pH 3 and 7, the uptake declines due to the presence of DOC in its zwitterionic form. Beyond pH 9, DOC species predominantly transform into anionic forms, leading to further reductions in adsorption due to electrostatic repulsion with the negatively charged CS–AC surface (Zhang et al., 2016b).

3.3 Effect of Initial AMX or DOC Concentration and Contact Time

The adsorption behavior of AMX and DOC at varying initial concentrations over time is depicted in Fig. 5. At each concentration level, a rapid increase in adsorption is observed during the initial phase, followed by a gradual decline in uptake until an equilibrium state is reached. This initial surge in adsorption can be attributed to the abundance of available adsorption sites on the CS–AC surface, facilitating efficient antibiotic molecule attachment. However, as adsorption progresses, the gradual saturation of active sites leads to a reduced rate of uptake until equilibrium is achieved (Tay et al., 2009). For both antibiotics, the equilibrium time is observed to be approximately 3 h for low initial concentrations (50 mg/L), around 9 h for moderate concentrations (100–200 mg/L), and extends to nearly 24 h for higher inlet concentrations (300–400 mg/L). This variation in equilibrium time is associated with the molecular diffusion process within the system. In more concentrated solutions, the higher density of antibiotic molecules restricts their mobility, reducing the diffusion rate and prolonging the time required to reach adsorption equilibrium (Pap et al., 2017). Additionally, an increase in the initial antibiotic concentration results in higher adsorption capacities, as a greater driving force is required to transport the antibiotic molecules toward the available adsorption sites on CS–AC. This phenomenon aligns with diffusion-controlled adsorption mechanisms, where greater solute concentrations create a stronger concentration gradient, enhancing mass transfer to the adsorbent surface (Kong et al., 2017). At saturation equilibrium, observed at approximately 23 h, the maximum adsorption capacities for AMX and DOC are determined to be 145 mg/g and 205 mg/g, respectively. These findings underscore the significant influence of initial antibiotic concentration on adsorption efficiency and the equilibrium time required for the system to reach saturation.

3.4 Isotherm Study of the Adsorption System

The correlation of the isotherm data, obtained using different equations, helps to assess the type and extent of adsorption. In this study, the Langmuir and Freundlich models were applied to the data as follows:

$$Q = \frac{Q_L C_e}{1 + K_L C_e} \tag{2}$$

$$Q = K_F C_e^{1/n} \tag{3}$$

where q_L (mg/g) represents the maximum antibiotic uptake, q_e (mg/g) indicates the amount of AMX or DOC adsorbed at equilibrium, C_e (mg/L) refers to the residual concentration of AMX or DOC in the liquid phase at equilibrium, K_L (L/mg) is the Langmuir constant, and n and K_F ((mg/g)(L/mg)^(1/n)) are the Freundlich parameters, which describe the strength and

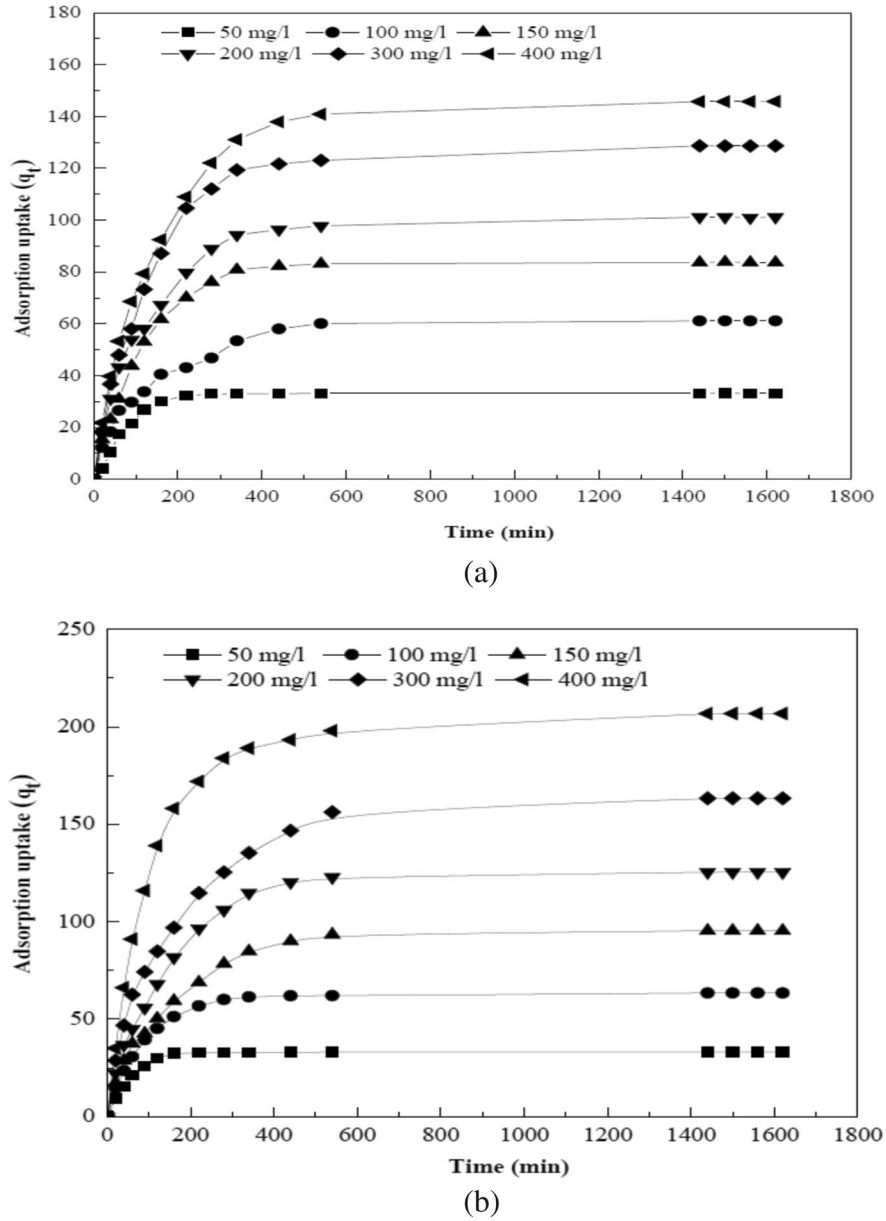

Fig. 5 Adsorption capacity over time at different initial antibiotic concentrations for (**a**) AMX and (**b**) DOC onto CS–AC (dosage: 1 g/L, agitation speed: 300 rpm, temperature: 30 °C)

extent of adsorption. To analyze the isotherm data, statistical regression was employed using the equations for the Langmuir and Freundlich models. The results revealed that the Langmuir model provided the best fit, with an R^2 value of 0.99 for both antibiotics, compared to R^2 values of 0.97 and 0.98 for AMX and DOC, respectively, when using the Freundlich model. The small discrepancies between the observed and predicted qe values for AMX were minimized by the Langmuir equation, with RMSE values ranging from 0.23 to 0.51, which were lower than those obtained using the Freundlich isotherm. For DOC, the Langmuir model had RMSE values between 0.46 and 0.63, also lower than the values for the Freundlich model, which ranged from 0.59 to 0.78. The equilibrium data for both antibiotics at different temperatures were compared with the predicted data from the Langmuir and Freundlich models, as shown in Fig. 6. The Langmuir model demonstrated the best fit, suggesting that the adsorption of both AMX and DOC on the uniform CS–AC structure is consistent with monolayer coverage. The nature of the adsorption process can

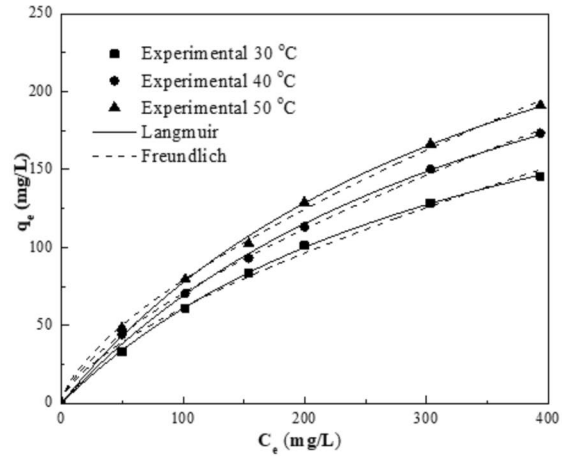

(a)

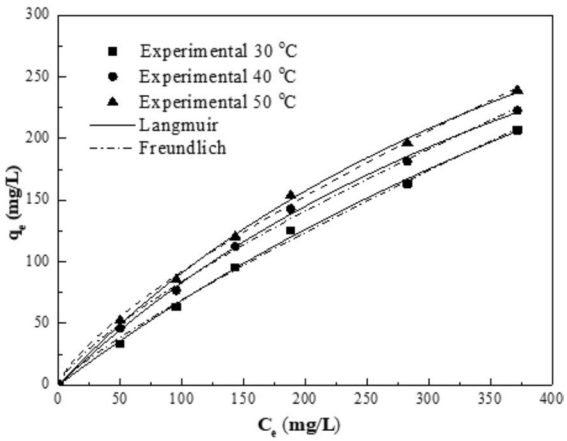

(b)

Fig. 6 The adsorption isotherms for (**a**) AMX and (**b**) DOC on CS–AC were modeled at varying temperatures to investigate the adsorption process

also be determined from the Freundlich constant (n), which is greater than 1, indicating favorable adsorption conditions. The highest uptake values calculated using the Langmuir constants were 161.36, 198.75, and 229.81 mg/g for AMX, and 235.09, 268.56, and 295.63 mg/g for DOC at 30, 40, and 50 °C, respectively. The increased antibiotic uptake observed in hot solutions indicates that the adsorption process is endothermic. Additionally, the adsorption capacity for DOC was found to be higher than that for AMX, which could be attributed to the greater hydrophobicity and larger molecular weight of DOC compared to AMX (Table 1). Finally, the maximum adsorption capacities of CS–AC for the antibiotics evaluated were compared with those of various other adsorbents from existing literature.

3.5 Kinetic Considerations of the Adsorption System

Predicting experimental kinetic data is essential for evaluating both the rate and nature of the adsorption process. To achieve this, the pseudo-second-order (PSO) and pseudo-first-order (PFO) models were applied to describe the uptake of antibiotics over time.

$$Q_t = Q_e\left[1 - e^{-k_1 t}\right] \tag{4}$$

$$Q_t = \frac{t}{\left[\frac{1}{k_2 Q_e^2}\right] + \left[\frac{t}{Q_e}\right]} \tag{5}$$

In these models, q_e (mg/g) represents the saturation adsorption capacity, q_t (mg/g) refers to the adsorption at any given time, and k_2 (g/mg.min) and k_1 (min^{-1})

Table 1 Isotherm analysis outcomes for AMX and DOC adsorption onto CS–AC at different solution temperatures

Temperature (°C)	Langmuir isotherm				Freundlich isotherm			
	qL (mg/g)	k_L(L/mg)	R^2	RMSE	k_F (mg/g) $(L/mg)^{1/n}$	n	R^2	RMSE
Amoxicillin								
30	161.36	0.027	0.99	0.51	30.69	1.54	0.97	0.59
40	198.75	0.024	0.99	0.28	43.17	1.51	0.98	0.37
50	229.81	0.026	0.99	0.23	58.61	1.53	0.97	0.42
Doxycycline								
30	235.09	0.007	0.99	0.63	53.34	1.19	0.98	0.78
40	268.56	0.010	0.99	0.46	67.48	1.33	0.98	0.64
50	295.63	0.011	0.99	0.47	71.41	1.37	0.98	0.59

Table 2 Pseudo-first-order and pseudo-second-order kinetic parameters for the adsorption of AMX and DOC onto CS–AC at 30 °C

C_0 (mg/l)	$q_{e,obs}$ (mg/g)	Pseudo-first-order				Pseudo-second-order			
		$q_{e,cal}$ (mg/g)	k_1 (/min)	R^2	RMSE	$q_{e,cal}$ (mg/g)	k_2 (g/mg min)	R^2	RMSE
Amoxicillin									
50	33.15	33.61	0.011	0.99	0.445	36.64	4.54E-04	0.95	1.315
100	61.15	60.16	0.007	0.99	1.022	66.45	1.48E-04	0.98	1.231
150	83.67	84.11	0.008	0.99	0.415	92.89	1.21E-04	0.97	2.467
200	101.17	100.11	0.008	0.99	1.117	110.46	9.89E-05	0.98	2.097
300	128.66	128.11	0.007	0.99	0.874	142.24	6.68E-05	0.98	3.378
400	145.75	147.97	0.007	0.99	1.876	163.98	5.52E-05	0.97	4.938
Doxycycline									
50	33.17	33.32	0.017	0.99	0.184	35.68	7.47E-04	0.96	0.886
100	63.47	62.92	0.011	0.99	0.317	68.57	2.33E-04	0.98	1.273
150	95.42	94.84	0.006	0.99	1.391	105.15	8.62E-05	0.98	2.162
200	125.44	125.38	0.007	0.99	1.180	139.14	6.65E-05	0.98	3.225
300	163.35	160.48	0.006	0.99	2.835	178.57	4.72E-05	0.97	3.522
400	206.87	202.57	0.009	0.99	1.523	223.25	5.76E-05	0.98	3.598

are the rate constants for the PSO and PFO models, respectively. Statistical regression analysis was employed to correlate the kinetic data with the equations for both the PSO and PFO models. The results indicate that the PFO model provides a more accurate fit for the data when compared to the PSO model, as evidenced by the higher R^2 values and lower RMSE values (Table 2). The plots of the measured and predicted *qt* values over time (*t*) for both AMX and DOC at various initial concentrations are presented in Fig. 7. For AMX adsorption, the PFO model displayed R^2 values as high as 0.99, compared to the PSO model, which ranged between 0.95 and 0.98. Additionally, the PFO model showed lower RMSE values (ranging from 0.415 to 1.876) compared to the PSO model (ranging from 1.231 to 4.938). Similarly, for DOC adsorption, the PFO model again demonstrated higher R^2 values (0.99) and lower RMSE values (0.184–2.835) than the PSO model, which had R^2 values of 0.96–0.98 and RMSE values between 0.886 and 3.598. These findings suggest that the PFO kinetic model is more suitable for describing the adsorption processes of both AMX and DOC on the CS–AC adsorbent. Moreover, it was observed that the magnitude of the PFO rate constant (*k1*) decreased as the amount of adsorbate increased. This phenomenon can be attributed to the increased competition for adsorption sites when higher amounts of antibiotics are present in the solution. This competition leads to a reduced adsorption rate and smaller *k1* values. Such behavior aligns with previous studies, where the PFO model successfully described the adsorption kinetics of tetracycline antibiotics onto activated carbon derived from human hair, demonstrating the model's broad applicability in understanding antibiotic adsorption systems. Overall, the results highlight the importance of selecting an appropriate kinetic model, with the PFO model proving to be more effective in characterizing the adsorption dynamics of AMX and DOC on CS–AC, and offering insights into the competitive interactions during the adsorption process.

In this study, adsorption kinetics were investigated in detail in order to reveal the rate of mass transfer in the system and the nature of the adsorption mechanism. The fact that the pseudo-first-order (PFO) model showed a higher correlation coefficient ($R^2 \approx 0.99$) and a lower root mean square error (RMSE) with the experimental data indicates that physical adsorption is dominant in the process.

However, not only macroscopic modeling was done, but also evaluations were made on the mechanisms limiting the adsorption process. The decrease in the adsorption rate with increasing initial antibiotic concentration shows that the active site competition in the system is effective and that adsorption is also limited by intraparticle diffusion. In parallel, the obtained data also allow for more advanced diffusion analyses. According to the intraparticle diffusion model, the adsorption process progresses in more than one stage:

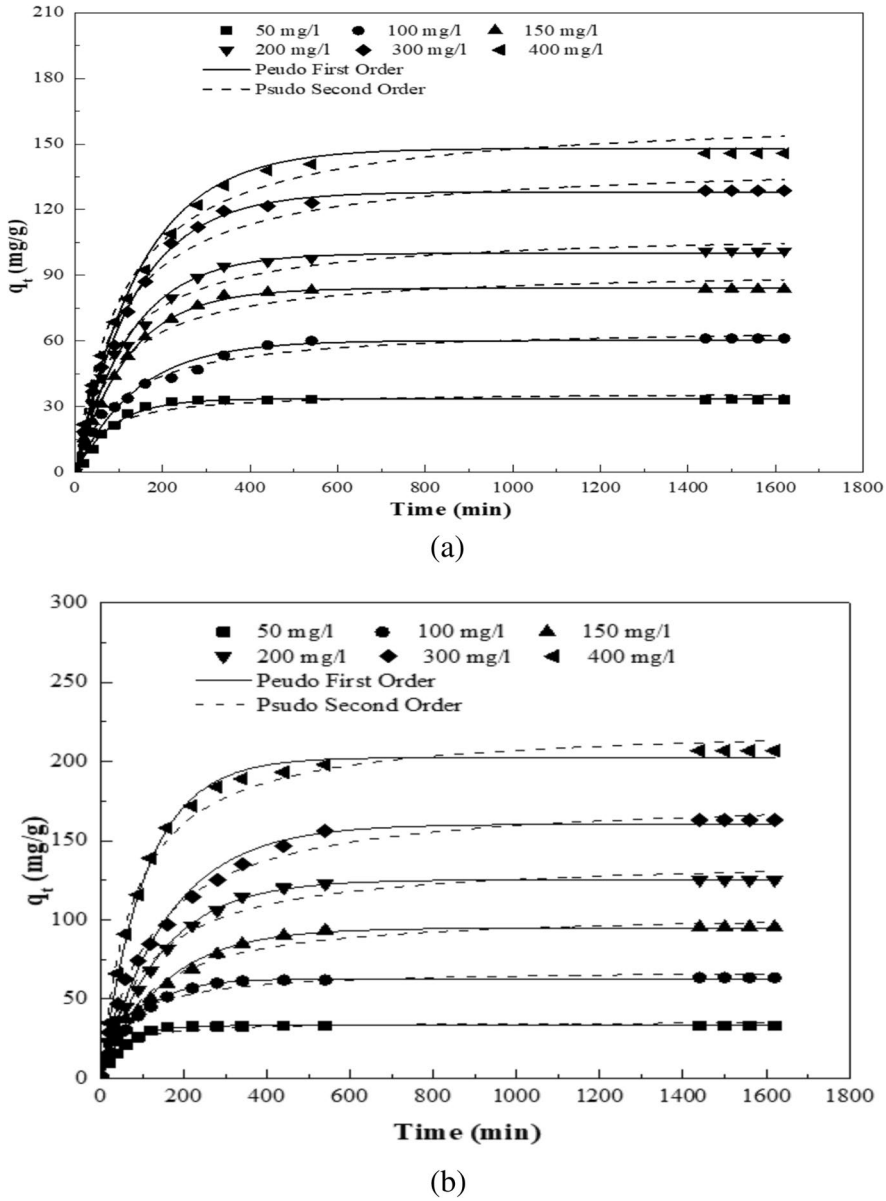

Fig. 7 Kinetic modeling of the adsorption of (**a**) AMX and (**b**) DOC onto CS–AC (dosage = 1 g/L, agitation rate = 300 rpm and 30 °C)

(i) boundary layer diffusion, (ii) intraparticle migration, and (iii) reaching equilibrium. This situation shows that the adsorption mechanism is not only composed of surface interactions; mass transfer resistances depending on the pore structure are also effective. In addition, it can be suggested to analyze the experimental data with the Boyd model. With this model, it can be determined more clearly whether the diffusion is limited by film diffusion or intraparticle diffusion. Especially, analyzing the interaction mechanisms of drugs with different molecular sizes and hydrophobicity levels such as AMX and DOC with the adsorbent surface through this model is important in terms of explaining the selectivity (Boyd et al., 1947; Foo & Hameed, 2010; Weber & Morris, 1963).

In conclusion, although the PFO kinetic model used in this study represents the experimental data well, the integration of multi-model analyses and diffusion-based kinetic evaluations is suggested for a more comprehensive understanding of the adsorption mechanism. This approach will provide more reliable data production in terms of system scalability and process optimization.

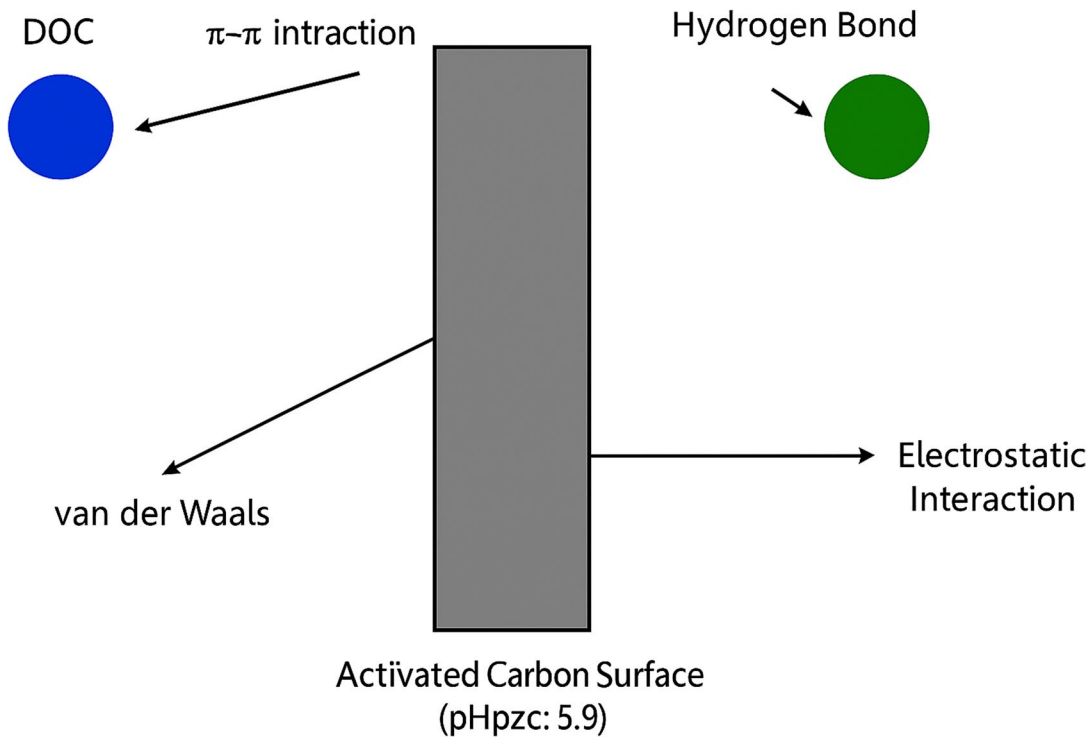

Fig. 8 Removal Mechanism

In response, we have conducted additional adsorption–desorption cycle experiments to evaluate the reusability of CS-AC. The adsorbent was subjected to five consecutive adsorption–desorption cycles using a mild eluent (ethanol/water mixture, 70:30 v/v) under optimized conditions.The adsorption capacity decreased by less than 12% after five cycles for both AMX and DOC, suggesting good structural stability and regeneration efficiency. The desorption efficiency remained above 85% throughout all cycles, which demonstrates the material's potential for repeated use without significant loss of performance. These new data significantly enhance the completeness of the study and support the potential of CS-AC as a cost-effective and regenerable biosorbent (Fig. 8).

4 Mechanism

Above, a scientific scheme of the removal mechanism performed by activated carbon is presented. This mechanism shows the interactions that are effective during the removal of antibiotics such as DOC (doxycycline) and AMX (amoxicillin).

4.1 Removal Mechanism Explanation

Zeta Potential (pHpzc ≈ 5.9): The surface charge of activated carbon changes depending on the pH. If pH <5.9, the surface is positive; if pH >5.9, it is negative. This affects the electrostatic interaction with AMX and DOC molecules in ionic form. π–π Interactions (DOC): The aromatic ring of DOC enters into π–π stacking interaction with the aromatic structure on the surface of activated carbon. Hydrogen Bonds (AMX):Hydrogen bonds are formed between the amino and carbonyl groups of AMX and the hydroxyl and carboxyl groups on the surface.

Van der Waals Forces:A weak but widespread attraction force is established between molecules and the porous carbon surface. Electrostatic Interactions: The positive or negative charge of the activated carbon surface, depending on the zeta potential, leads to electrostatic attraction or repulsion with the ionic

species of AMX and DOC. Chemical Mechanisms of H_3PO_4 Activation:

A detailed explanation has been added describing how phosphoric acid promotes microporosity through chemical pathways such as: Dehydration of hydroxyl groups, Cleavage of glycosidic bonds, Formation of phosphate bridges, Cross-linking of biopolymer chains during activation.

We have now included a direct quantitative comparison of CS-AC with other chitosan-derived and biomass-based activated carbons from recent literature, focusing on adsorption capacity for antibiotics (AMX and DOC), BET surface area, and preparation yield. The results indicate that CS-AC exhibits a higher adsorption capacity. Our synthesis route involves a single-step activation process without pre-carbonization or complex chemical modification, offering a low-energy and scalable pathway. Unlike many prior studies focusing on either AMX or DOC separately, our study explores the removal of both antibiotics using a single biosorbent under a broad range of conditions. This dual-target scope enhances the environmental relevance of the adsorbent. We employed a broader suite of characterization techniques (e.g., FTIR, BET, SEM, pHpzc) and linked the physicochemical properties of CS-AC to adsorption behavior, enabling deeper mechanistic insight, especially on π–π interactions and H-bonding for DOC and AMX, respectively. These improvements and clarifications have been integrated into the revised manuscript to better articulate the novelty and contribution of our work in the context of current literature.

Chitosan is derived from crustacean waste (e.g., shrimp shells), an abundant and renewable biopolymer, requiring minimal pretreatment, unlike lignocellulosic or synthetic materials. Phosphoric acid activation is performed under relatively low temperature (~ 400–500 °C), reducing energy consumption compared to other physical or chemical activation methods (e.g., KOH or $ZnCl_2$-based activation). Unlike commercial activated carbons, which may require multi-step processing and expensive precursors, our CS-AC synthesis utilizes a single-step acid activation method without the need for toxic or corrosive chemicals, enhancing environmental safety and lowering operational costs. Preliminary cost comparison suggests that the material cost per gram of CS-AC is at least 30–50% lower than that of commercial activated carbons, when raw materials and energy input are considered.

5 Conclusions

The CS–AC adsorbent, which was synthesized via a one-step H_3PO_4 activation method, demonstrated a significantly higher surface area of 998.02 m^2/g, indicative of its enhanced porosity and surface characteristics. The adsorbent exhibited multi-functional adsorption sites, which were further supported by its well-developed pore structure. Specifically, the CS–AC had a pore volume of 0.485 cm^3/g and an average pore size of 2.05 nm, making it highly suitable for adsorption applications. These surface and textural properties contributed to the efficient removal of antibiotics, namely AMX (Amoxicillin) and DOC (Doxycycline), from aqueous solutions. The adsorption data obtained for both AMX and DOC were effectively modeled using the Langmuir and Pseudo-First-Order (PFO) adsorption isotherms, which provided a reliable framework for describing the interaction between the adsorbent and the target antibiotics. The Langmuir isotherm, in particular, suggested a monolayer adsorption on a surface with a finite number of identical adsorption sites, while the PFO model described the adsorption kinetics, aligning well with the experimental data. At an elevated temperature of 50 °C, CS–AC demonstrated outstanding adsorption capacities of 229.81 mg/g for AMX and 295.63 mg/g for DOC, reflecting the high adsorption efficiency of the material at this temperature. These results indicate that CS–AC is a highly effective adsorbent for the removal of both AMX and DOC from aqueous solutions, showing great potential for practical applications in water treatment and pharmaceutical waste management. In conclusion, CS–AC, with its favorable surface area, pore volume, and functional sites, presents a promising solution for the adsorption of antibiotics like AMX and DOC, making it a viable option for addressing contamination in water bodies and promoting environmental sustainability.

Acknowledgements Çanakkale Onsekiz Mart University and Çankırı Karatekin University are thanked in this article for their analysis, testing, and laboratory facilities.

Author Contribution **Feride N. Türk:** Writing, Acquisition of data, Analysis of data, Approval of the version of the manuscript to be published, review and editing, **Hasan Arslanoğlu:** Writing, Revising the manuscript critically for important intellectual content, Approval of the version of the manuscript to be published, review and editing.

Funding Open access funding provided by the Scientific and Technological Research Council of Türkiye (TÜBİTAK). This study was supported by the ÇOMÜ Scientific Research Projects Commission with the project numbered FHD-2024–4769.

Data Availability The data that support the findings of this study are available from the corresponding author, upon reasonable request.

Code Availability Not applicable.

Declarations

Ethics Approval Not applicable.

Consent to Participate Not applicable.

Consent for Publication Not applicable.

Competing interest The authors declare that there are no conflicts of interest regarding the publication of this paper.

References

Ahamad, T., Naushad, M., Al-Shahrani, T., Al-Hokbany, N., & Alshehri, S. M. (2020). Preparation of chitosan based magnetic nanocomposite for tetracycline adsorption: Kinetic and thermodynamic studies. *International Journal of Biological Macromolecules, 147*, 258–267.

Antonelli, R., Malpass, G. R. P., da Silva, M. G. C., & Vieira, M. G. A. (2020). Adsorption of ciprofloxacin onto thermally modified bentonite clay: Experimental design, characterization, and adsorbent regeneration. *Journal of Environmental Chemical Engineering, 8*(6), Article 104553.

Avcı, A., İnci, İ, & Baylan, N. (2020). Adsorption of ciprofloxacin hydrochloride on multiwall carbon nanotube. *Journal of Molecular Structure, 1206*, Article 127711.

Baccar, R., Sarrà, M., Bouzid, J., Feki, M., & Blánquez, P. (2012). Removal of pharmaceutical compounds by activated carbon prepared from agricultural by-product. *Chemical Engineering Journal, 211*, 310–317.

Bagheri, H., Afkhami, A., & Noroozi, A. (2016). Removal of pharmaceutical compounds from hospital wastewaters using nanomaterials: A review. *Analytical and Bioanalytical Chemistry Research, 3*(1), 1–18.

Bhatnagar, A., & Sillanpää, M. (2010). Utilization of agro-industrial and municipal waste materials as potential adsorbents for water treatment—A review. *Chemical Engineering Journal, 157*(2–3), 277–296. https://doi.org/10.1016/j.cej.2010.01.007

Boudrahem, N., Delpeux-Ouldriane, S., Khenniche, L., Boudrahem, F., Aissani-Benissad, F., & Gineys, M. (2017). Single and mixture adsorption of clofibric acid, tetracycline and paracetamol onto activated carbon developed from cotton cloth residue. *Process Safety and Environmental Protection, 111*, 544–559.

Boyd, G. E., Adamson, A. W., & Myers, L. S. (1947). The exchange adsorption of ions from aqueous solutions by organic zeolites. II. Kinetics. *Journal of the American Chemical Society, 69*(11), 2836–2848. https://doi.org/10.1021/ja01202a066

Brigante, M., & Avena, M. (2016). Biotemplated synthesis of mesoporous silica for doxycycline removal. Effect of pH, temperature, ionic strength and Ca2+ concentration on the adsorption behaviour. *Microporous and Mesoporous Materials, 225*, 534–542.

Cella, D. F., Tulsky, D. S., Gray, G., Sarafian, B., Linn, E., Bonomi, A., & Brannon, J. (1993). The Functional Assessment of Cancer Therapy scale: Development and validation of the general measure. *Journal of Clinical Oncology, 11*(3), 570–579.

Chao, Y., Zhu, W., Wu, X., Hou, F., Xun, S., Wu, P., & Li, H. (2014). Application of graphene-like layered molybdenum disulfide and its excellent adsorption behavior for doxycycline antibiotic. *Chemical Engineering Journal, 243*, 60–67.

Chayid, M. A., & Ahmed, M. J. (2015). Amoxicillin adsorption on microwave prepared activated carbon from Arundo donax Linn: Isotherms, kinetics, and thermodynamics studies. *Journal of Environmental Chemical Engineering, 3*(3), 1592–1601.

da Silva Alves, D. C., Healy, B., Pinto, L. A. D. A., Cadaval, T. R. S. A., Jr., & Breslin, C. B. (2021). Recent developments in chitosan-based adsorbents for the removal of pollutants from aqueous environments. *Molecules, 26*(3), 594.

Fan, X., Zhang, L., Zhang, G., Shu, Z., & Shi, J. (2013). Chitosan derived nitrogen-doped microporous carbons for high performance CO2 capture. *Carbon, 61*, 423–430.

Fan, H., Ma, Y., Wan, J., Wang, Y., Li, Z., & Chen, Y. (2020). Adsorption properties and mechanisms of novel biomaterials from banyan aerial roots via simple modification for ciprofloxacin removal. *Science of the Total Environment, 708*, Article 134630.

Foo, K. Y., & Hameed, B. H. (2010). Insights into the modeling of adsorption isotherm systems. *Chemical Engineering Journal, 156*(1), 2–10. https://doi.org/10.1016/j.cej.2009.09.013

Foo, K. Y., & Hameed, B. H. (2012). Preparation and characterization of activated carbon from pistachio nut shells via microwave-induced chemical activation. *Biomass*

and Bioenergy, 46, 257–262. https://doi.org/10.1016/j.biombioe.2012.08.004

Freundlich, H. (1907). Über die Adsorption in Lösungen. *Z Für Phys Chem, 57U*, 385–470.

Gao, Y., Li, Y., Zhang, L., Huang, H., Hu, J., Shah, S. M., & Su, X. (2012). Adsorption and removal of tetracycline antibiotics from aqueous solution by graphene oxide. *Journal of Colloid and Interface Science, 368*(1), 540–546.

Gunawardene, O. H., Gunathilake, C. A., Vikrant, K., & Amaraweera, S. M. (2022). Carbon dioxide capture through physical and chemical adsorption using porous carbon materials: A review. *Atmosphere, 13*(3), 397.

Ho, Y. S., & McKay, G. (1999). Pseudo-second order model for sorption processes. *Process Biochemistry, 34*(5), 451–465. https://doi.org/10.1016/S0032-9592(98)00112-5

Ioannidou, O., & Zabaniotou, A. (2007). Agricultural residues as precursors for activated carbon production—A review. *Renewable and Sustainable Energy Reviews, 11*(9), 1966–2005. https://doi.org/10.1016/j.rser.2006.03.013

Kerkez-Kuyumcu, Ö., Bayazit, ŞS., & Salam, M. A. (2016). Antibiotic amoxicillin removal from aqueous solution using magnetically modified graphene nanoplatelets. *Journal of Industrial and Engineering Chemistry, 36*, 198–205.

Kimura, K., Hara, H., & Watanabe, Y. (2005). Removal of pharmaceutical compounds by submerged membrane bioreactors (MBRs). *Desalination, 178*(1–3), 135–140.

Kong, Q., He, X., Shu, L., & Miao, M. S. (2017). Ofloxacin adsorption by activated carbon derived from luffa sponge: Kinetic, isotherm, and thermodynamic analyses. *Process Safety and Environmental Protection, 112*, 254–264.

Kumar, A., Patra, C., Rajendran, H. K., & Narayanasamy, S. (2022). Activated carbon-chitosan based adsorbent for the efficient removal of the emerging contaminant diclofenac: Synthesis, characterization and phytotoxicity studies. *Chemosphere, 307*, Article 135806.

Kümmerer, K. (2009). Antibiotics in the aquatic environment–A review–Part I. *Chemosphere, 75*(4), 417–434. https://doi.org/10.1016/j.chemosphere.2008.11.086

Lagergren, S. (1898). Zur theorie der sogenannten adsorption geloster stoffe. *Kungliga Svenska Vetenskapsakademiens. Handlingar, 24*, 1–39.

Langmuir, I. (1916). The constitution and fundamental properties of solids and liquids. Part I. Solids. *Journal of the American Chemical Society, 38*(11), 2221–2295.

Liu, S., Xu, W. H., Liu, Y. G., Tan, X. F., Zeng, G. M., Li, X., & Cai, X. X. (2017). Facile synthesis of Cu (II) impregnated biochar with enhanced adsorption activity for the removal of doxycycline hydrochloride from water. *Science of the Total Environment, 592*, 546–553.

Liu, Y., Zhao, Y., Li, K., Wang, Z., Tian, P., Liu, D., & Wang, J. (2018). Activated carbon derived from chitosan as air cathode catalyst for high performance in microbial fuel cells. *Journal of Power Sources, 378*, 1–9.

Liu, X. Q., Zhao, X. X., Liu, Y., & Zhang, T. A. (2022). Review on preparation and adsorption properties of chitosan and chitosan composites. *Polymer Bulletin, 79*(4), 2633–2665.

Lu, T., Zhu, Y., Qi, Y., Wang, W., & Wang, A. (2018). Magnetic chitosan–based adsorbent prepared via Pickering high internal phase emulsion for high-efficient removal of antibiotics. *International Journal of Biological Macromolecules, 106*, 870–877.

Mangla, D., Sharma, A., & Ikram, S. (2022). Critical review on adsorptive removal of antibiotics: Present situation, challenges and future perspective. *Journal of Hazardous Materials, 425*, Article 127946.

Martínez-Carballo, E., González-Barreiro, C., Scharf, S., & Gans, O. (2007). Environmental monitoring study of selected veterinary antibiotics in animal manure and soils in Austria. *Environmental Pollution, 148*(2), 570–579. https://doi.org/10.1016/j.envpol.2006.11.035

Martins, M., Mourato, C., Sanches, S., Noronha, J. P., Crespo, M. B., & Pereira, I. A. (2017). Biogenic platinum and palladium nanoparticles as new catalysts for the removal of pharmaceutical compounds. *Water Research, 108*, 160–168.

Marzbali, M. H., Esmaieli, M., Abolghasemi, H., & Marzbali, M. H. (2016). Tetracycline adsorption by H3PO4-activated carbon produced from apricot nut shells: A batch study. *Process Safety and Environmental Protection, 102*, 700–709.

Moussavi, G., Alahabadi, A., Yaghmaeian, K., & Eskandari, M. (2013). Preparation, characterization and adsorption potential of the NH4Cl-induced activated carbon for the removal of amoxicillin antibiotic from water. *Chemical Engineering Journal, 217*, 119–128.

Naeimi, S., & Faghihian, H. (2017). Application of novel metal organic framework, MIL-53 (Fe) and its magnetic hybrid: For removal of pharmaceutical pollutant, doxycycline from aqueous solutions. *Environmental Toxicology and Pharmacology, 53*, 121–132.

Naghdi, M., Taheran, M., Brar, S. K., Kermanshahi-Pour, A., Verma, M., & Surampalli, R. Y. (2018). Removal of pharmaceutical compounds in water and wastewater using fungal oxidoreductase enzymes. *Environmental Pollution, 234*, 190–213.

Pap, S., Knudsen, T. Š, Radonić, J., Maletić, S., Igić, S. M., & Sekulić, M. T. (2017). Utilization of fruit processing industry waste as green activated carbon for the treatment of heavy metals and chlorophenols contaminated water. *Journal of Cleaner Production, 162*, 958–972.

Putra, E. K., Pranowo, R., Sunarso, J., Indraswati, N., & Ismadji, S. (2009). Performance of activated carbon and bentonite for adsorption of amoxicillin from wastewater: Mechanisms, isotherms and kinetics. *Water Research, 43*(9), 2419–2430.

Rocha, L. S., Pereira, D., Sousa, É., Otero, M., Esteves, V. I., & Calisto, V. (2020). Recent advances on the development and application of magnetic activated carbon and char for the removal of pharmaceutical compounds from waters: A review. *Science of the Total Environment, 718*, Article 137272.

Sánchez-Polo, M., Rivera-Utrilla, J., Prados-Joya, G., Ferro-García, M. A., & Bautista-Toledo, I. (2008). Removal of pharmaceutical compounds, nitroimidazoles, from waters by using the ozone/carbon system. *Water Research, 42*(15), 4163–4171.

Sayğılı, H., & Güzel, F. (2016). Effective removal of tetracycline from aqueous solution using activated carbon

prepared from tomato (Lycopersicon esculentum Mill.) industrial processing waste. *Ecotoxicology and Environmental Safety, 131*, 22–29.

Sun, Yuanyuan, et al. (2016). Characterization and ciprofloxacin adsorption properties of activated carbons prepared from biomass wastes by H3PO4 activation. *Bioresource Technology, 217*, 239–244.

Tambosi, J. L., de Sena, R. F., Favier, M., Gebhardt, W., José, H. J., Schröder, H. F., & Moreira, R. D. F. P. M. (2010). Removal of pharmaceutical compounds in membrane bioreactors (MBR) applying submerged membranes. *Desalination, 261*(1–2), 148–156.

Tay, T., Ucar, S., & Karagöz, S. (2009). Preparation and characterization of activated carbon from waste biomass. *Journal of Hazardous Materials, 165*(1–3), 481–485.

Tien, C., & Ramarao, B. V. (2017). On the significance and utility of the Lagergren model and the pseudo second-order model of batch adsorption. *Separation Science and Technology, 52*(6), 975–986.

Tiwari, B., Sellamuthu, B., Ouarda, Y., Drogui, P., Tyagi, R. D., & Buelna, G. (2017). Review on fate and mechanism of removal of pharmaceutical pollutants from wastewater using biological approach. *Bioresource Technology, 224*, 1–12.

Tseng, R. L. (2006). Mesopore control of high surface area NaOH-activated carbon. *Journal of Colloid and Interface Science, 303*(2), 494–502.

Watkinson, A. J., Murby, E. J., & Costanzo, S. D. (2007). Removal of antibiotics in conventional and advanced wastewater treatment: Implications for environmental discharge and wastewater recycling. *Water Research, 41*(18), 4164–4176. https://doi.org/10.1016/j.watres.2007.04.005

Weber, W. J., & Morris, J. C. (1963). Kinetics of adsorption on carbon from solution. *Journal of the Sanitary Engineering Division, 89*(2), 31–60.

Wróbel-Iwaniec, I., Díez, N., & Gryglewicz, G. (2015). Chitosan-based highly activated carbons for hydrogen storage. *International Journal of Hydrogen Energy, 40*(17), 5788–5796.

Yang, S., Zhang, Z., Wang, H., & Jia, H. (2019). Adsorption of tetracycline antibiotics from an aqueous solution onto graphene oxide/calcium alginate composite fibers. *RSC Advances, 9*(13), 7072–7083. https://doi.org/10.1039/C8RA09014E

Zhang, D. Q., Tan, S. K., Gersberg, R. M., Sadreddini, S., Zhu, J., & Tuan, N. A. (2011). Removal of pharmaceutical compounds in tropical constructed wetlands. *Ecological Engineering, 37*(3), 460–464.

Zhang, S., Dong, Y., Yang, Z., Yang, W., Wu, J., & Dong, C. (2016a). Adsorption of pharmaceuticals on chitosan-based magnetic composite particles with core-brush topology. *Chemical Engineering Journal, 304*, 325–334.

Zhang, X., Bai, B., Puma, G. L., Wang, H., & Suo, Y. (2016b). Novel sea buckthorn biocarbon SBC@ β-FeOOH composites: Efficient removal of doxycycline in aqueous solution in a fixed-bed through synergistic adsorption and heterogeneous Fenton-like reaction. *Chemical Engineering Journal, 284*, 698–707.

Zhang, X., Liu, Y., Gao, B., & Xu, H. (2020). Adsorption mechanisms of amoxicillin on biochars derived from rice husk and wheat straw. *Environmental Pollution, 256*, Article 113343. https://doi.org/10.1016/j.envpol.2019.113343

Zhao, L., Yao, J., Gao, M., & Jin, H. (2022). Enhanced adsorption of doxycycline by functionalized biochar with abundant π-electrons and oxygen-containing groups. *Chemosphere, 286*, Article 131710. https://doi.org/10.1016/j.chemosphere.2021.131710